Air conditioning of a low ceiling operating theaters

Medhat M. Sorour, Mohamed A. Teamah and Mohamed G. Ghorab
Mechanical Eng. Dept., Faculty of Eng., Alexandria University, Alexandria, Egypt

This numerical study is devoted to compute the airflow patterns, velocity and temperature profiles inside an operating theater with low ceiling. The flow is assumed to be laminar two-dimensional. The conducted mathematical model was solved using finite volume technique. The investigated design parameters were the effect of inlet and outlet slots location as well as the hang partition. The operating parameters were the Reynolds number and heat source. The study covers a wide range for Reynolds number from zero (stagnant condition) to 10^4 and heat generation ratio from 0.075 to 0.15. A comparison was made with previous investigations, a good agreement was found. Optimum design and operating parameters were concluded. Finally, Design charts were constructed and a case study was exampled.

البحث يتناول دراسة عددية لحركة ودرجة حرارة الهواء المكيف في غرف عمليات ذات سقوف منخفضة. وخلال البحث تم استنباط نموذج رياضى وحل النموذج الرياضى وقد تم حساب ورسم خرائط لسرعات الهواء وخطوط السريان وخطوط ثبات درجات الحرارة في الحالات المختلفة لمداخل ومخارج الهواء وأماكن تعليق العوارض وحجم العوارض لقيم مختلفة لرقم رينولدز وكذلك لقيم شدة توليد الطاقة الحرارية المتولدة من المصادر الحرارية داخل هذه الغرف مثل الإضاءة والمعدات الطبية وكذلك الأشخاص. وقد شملت الدراسة حالات لمواضع الدخول والخروج ومكان وحجم العارض. وقد تم الاستعانة بالابعاد الحقيقية والاماكن المختلفة للمعدات الطبية وقيمة التوليد الحرارى لهذة المعدات من احدى غرف العمليات بمستشفى الطلبة الجامعى بجامعة الاسكندرية. وغطت الدراسة مدي واسع لرقم رينولدز من ١٠٠ الي ١٠٠٠٠ وقيمة نسبة حرارة تعادل من صفر وحتى ٠,١٥ وقد تم اعداد خرائط تصميمية لربط مدخل الهواء بسرعة الهواء المطلوبة وبمعرفة معدل التولبد الحرارى يمكن التنبؤ بقيمة درجة الحرارة التى يتعرض لها المريض. ويمكن استخدام هذة الخرائط فى تصميم واختيار اجهزة التكييف.

Keywords: Air flow, Air conditioning, Low ceiling, Heat transfer, Patankar and spalding technique

1. Introduction

The prediction of air movement in space is one of the most challenging tasks for the designer of 'HVAC' systems. Room air movement is a complicated process. It is determined by the building geometry, inlet diffuser configuration and location, exhaust (return) location, air velocity, ventilation rate, internal obstruction, and thermal buoyancy due to the heat generated by occupants and /or equipment. Studies of operating theater air distribution devices and observation of installations in industrial clean rooms indicate the delivery of the air from the ceiling. Downward movement from several supply inlets is probably the most effective air movement pattern. Completely perforated ceilings, partially perforated ceilings, and ceiling mounted diffusers have been applied successfully. Surgical operating theatre suites are typically in use no more than 8 to 12 hr /day. In general, outlets supplying air to sensitive ultra clean areas should be located on ceiling, while several exhaust outlets should be near the floor. The unidirectional laminar airflow pattern is commonly attained at velocity of 0.45 ±0.10 m/s. laminar air flow has shown satisfactory results for patient. On the other hand, an increasing number of private hospitals are being built in ordinary buildings where the height is limited to 3 meters. An ordinary air supply from ceiling will further reduce the height by approximately 0.5 m, for distribution making it unsuitable. The propose of this study is to investigate the possibility of inlet supply from sidewall in an operating theater and compare between these studies with the basic case supply from ceiling in buildings with height greater than 3 meter.

The general subject of air distribution in confined spaces was studied in the early 70's, Miller and Nash [1], Miller and Nevins [2]. One result of their work was the development of the Air Distribution Performance Index

(ADPI), which is widely used as a design criterion for selection of air handling equipment. Nielson [3] was one of the first to predict air movement and heat transfer in building using Computational Fluid Dynamics (CFD) methods. He developed a calculation procedure based on a stream function approach for predicting two dimensional flow patterns in ventilated rooms. Nielson et al. [4] used a finite volume solution of the two dimensional equations for the conservation of mass, momentum, and energy as well as the two k-ε equations for turbulence structure. Baker et al. [5] addressed certain benchmark investigation on the validation of CFD procedures for room air motion. They have achieved significant contribution in the history of CFD application in building engineering with inner heat source. Vazquez et al. [6] performed a numerical study of the ventilation patterns inside an auditorium of the University of Mexico. Jiang et al. [7] presented a numerical simulation of airflow pattern, temperature distribution, and percentage of dissatisfied people in a two-zone enclosure with mixed concentration conditions. Control of airborne particle concentration, and draught risk in an operating room, was investigated by Chen et al. [8].

Designing HVAC systems for optimum indoor air quality was studied by Lizardos [9] Vazquez et al. [10] studied the ventilation of an auditorium and its effect on wall heat transfer. A program CFD, with the k-ε model was used for the representation of turbulence. Kruger [11] studied temperature and velocity distributions from slot devices, and also studied the effect of the internal heating in a device on the thermal comfort, where the ventilation systems and air supply devices have to be used in different kinds of buildings depending on the demands regarding the size and location of the occupation zone and the need for outdoor air flow rates. The highest air velocities and the lowest air temperatures in the occupation zone will often occur close to inlet air devices. Nho et al. [12] studied numerically the airflow system with heat sources in an indoor telecommunication room. Xiaoxiong et al. [13]. Studied the effect of the different parameters on performance of the displacement ventilation system introducing the impact of heat source type, position, and wall characteristics on the temperature distribution. Fahim [14] studied by using experimental measurements (full-scale model) and numerical model, the parameter affecting the air distribution inside air-condition room. He optimized room comfort condition, and his analysis of airflow was turbulent in nature with the aid of detailed measurements of local values of velocity fluctuations.

In 2000, Sinha et al. [15], investigated numerical simulation of two-dimensional room airflow with and without buoyancy. Castanet et al. [16] studied the ventilation efficiency under some typical airflow conditions in a mechanically ventilated room. The study deals with indoor air quality and was mainly based on an experimental work full-scale test. In 2004, Khalil [17] investigated experimentally and numerically the airflow properties and heat exchange in the surgical operating theatres. The experimental study was carried out in an actual surgical operating theatre and the numerical procedure was three-dimensional using CFD model to determine the airflow characteristics, turbulence intensities, and air temperature and relative humidity distribution in the surgical operating theatres under various design and operation condition.

2. Mathematical modeling

The fluid inside the space will be considered a Newtonian, incompressible fluid (constant property fluid) except for the density in the buoyancy force components existing in the momentum equations. The Boussinesq approximation will relate the density to local temperature.

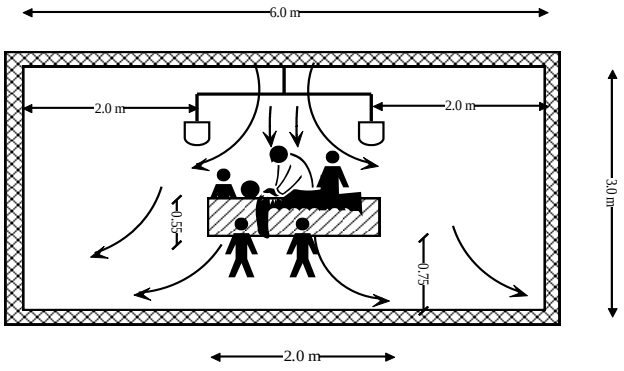

Fig. 1. Operating room configuration.

The steady state two dimensional governing Equations are:

$$\frac{\partial u}{\partial x}+\frac{\partial v}{\partial y}=0\,, \tag{1}$$

$$u\frac{\partial u}{\partial x}+v\frac{\partial u}{\partial y}=-\frac{1}{\rho}\frac{\partial p}{\partial x}+\nu\left(\frac{\partial^2 u}{\partial x^2}+\frac{\partial^2 u}{\partial y^2}\right), \tag{2}$$

$$u\frac{\partial v}{\partial x}+v\frac{\partial v}{\partial y}=-\frac{1}{\rho}\frac{\partial p}{\partial y}+\nu\left(\frac{\partial^2 v}{\partial x^2}+\frac{\partial^2 v}{\partial y^2}\right), \tag{3}$$

$$\rho c\left(u\frac{\partial \mathrm{T}}{\partial x}+\nu\frac{\partial \mathrm{T}}{\partial y}\right)=q''+K\left(\frac{\partial^2 T}{\partial x^2}+\frac{\partial^2 T}{\partial y^2}\right). \tag{4}$$

Where: -

$$-\frac{\partial p}{\partial y}=g\,(\rho-\rho_\infty). \tag{5}$$

It is possible to eliminate the local density in the momentum eq. (3) in favor of the local temperature through the definition of the coefficient of volumetric thermal expansion of the fluid:

$$\beta=-\frac{1}{\rho}\left(\frac{\partial \rho}{\partial T}\right)_p\,. \tag{6}$$

For moderate variation in temperature, the derivation in the above equation can be linearized as:

$$\left(\frac{\partial \rho}{\partial T}\right)_p=\left(\frac{\rho-\rho_\infty}{T-T_\infty}\right). \tag{7}$$

$$\therefore(\rho-\rho_\infty)=-\rho\beta(\mathrm{T}-\mathrm{T}_\infty)\,. \tag{8}$$

Introducing the following dimensionless variables:

$$X^*=\frac{x}{h}\,,\quad Y^*=\frac{y}{h}\,,\quad U^*=\frac{u}{U_i}\,,\quad V^*=\frac{v}{U_i}\,,$$
$$P^*=\frac{p}{\rho U_i^{\,2}}\,,\quad \theta=\frac{T-T_i}{T_l-T_i}\,,\ \text{and}\quad q^*=\frac{q''h}{U_i^{\,3}\rho} \tag{9}$$

Substituting the dimensionless variable of eq. (9) into the continuity eq. (1), momentum eqs. (2, 3) and energy eq. (4), we get.

$$\frac{\partial U^*}{\partial X^*}+\frac{\partial V^*}{\partial Y^*}=0\,. \tag{10}$$

$$U^*\frac{\partial U^*}{\partial X^*}+V^*\frac{\partial U^*}{\partial Y^*}=\frac{1}{\mathrm{Re}}\left(\frac{\partial^2 U^*}{\partial X^{*2}}+\frac{\partial^2 U^*}{\partial Y^{*2}}\right)-\frac{\partial P^*}{\partial X^*}\,. \tag{11}$$

$$U^*\frac{\partial V^*}{\partial X^*}+V^*\frac{\partial V^*}{\partial Y^*}=\frac{1}{\mathrm{Re}}\left(\frac{\partial^2 V^*}{\partial X^{*2}}+\frac{\partial^2 V^*}{\partial Y^{*2}}\right)-\frac{\partial P^*}{\partial Y^*}\,. \tag{12}$$

$$U^*\frac{\partial \theta}{\partial X^*}+V^*\frac{\partial \theta}{\partial Y^*}=$$
$$H.R.+\frac{1}{\mathrm{Re}^*\,\mathrm{Pr}}\left(\frac{\partial^2 \theta}{\partial X^{2^*}}+\frac{\partial^2 \theta}{\partial Y^{2^*}}\right). \tag{13}$$

Where Re, H.R. and Pr are Reynolds number, heat ratio, and Prandtl number respectively.
Where:

$H.R. = q'' / (U\rho\Delta T/h)$ or $H.R = q'' / (\Delta H/h^2)$

2.1. Boundary conditions

Fig. 2 illustrates the boundary conditions for operating room with supply from sidewall and exit from opposite wall near the floor, the exit temperature from the space must be calculated by applying conservation of energy.

$$\Sigma\, Q_{in}=\Sigma\, Q_{out}\,. \tag{14}$$

Q_{in} = the energy of air at inlet and the energy consumption from internal heat source.
Q_{out} = the energy of air at exit from space.

$$T_i+\frac{K}{\dot{m}_i C}\left(dx^*\frac{\partial T}{\partial y}+dy^*\frac{\partial T}{\partial x}\right)=T_o\,. \tag{15}$$

Where $\dot{m}_i=\dot{m}_o$, $\dot{m}_i=\rho U_i h^*1$

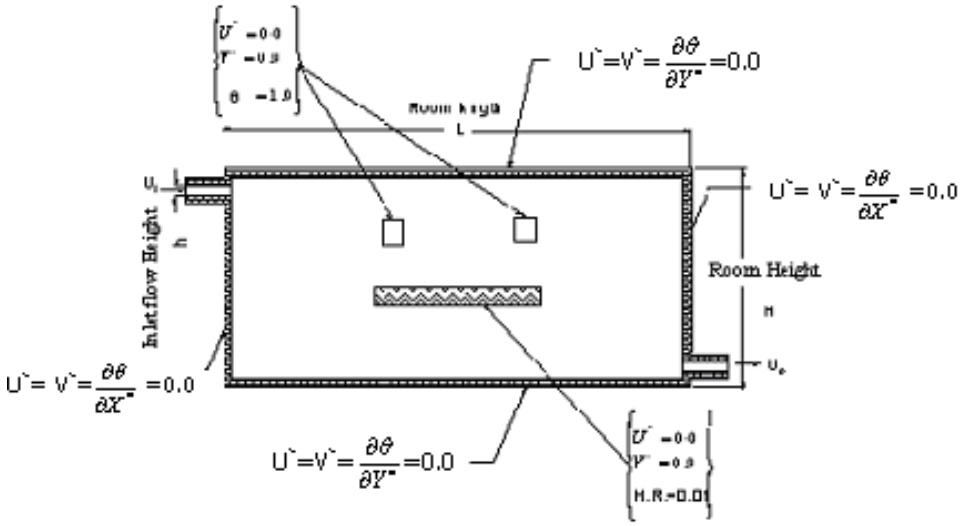

Fig. 2. Boundary conditions.

$$\therefore \mathrm{Re} = \frac{\rho U_i h}{\mu} = \frac{\dot{m}_i}{\mu}. \quad (16)$$

Introducing the dimensionless variable from eq. (9) and eq. (16) in eq. (15)

$$\theta_i + \frac{K}{\mathrm{Re}^* \mu^* C}\left(dX^* * \frac{\partial\theta}{\partial Y^*} + dY^* * \frac{\partial\theta}{\partial X^*}\right) = \theta_o. \quad (17)$$

$$\theta_o = \theta_i + \frac{1}{\mathrm{Re}^* \mathrm{Pr}} \sum\left(dX^* * \frac{\partial\theta}{\partial Y^*} + dY^* * \frac{\partial\theta}{\partial X^*}\right). \quad (18)$$

$$\left.\begin{array}{l} U^*=V^*=\dfrac{\partial\theta}{\partial Y^*}=0.0, \text{ At } Y^*=0.0 \text{ and } H/h \\ U^*=V^*=\dfrac{\partial\theta}{\partial X^*}=0.0, \text{ At } X^*=0.0 \text{ and} \\ 0.0< Y^* < \dfrac{H-h}{h} \\ U^*=1.0 \text{ and } V^*=\theta_i=0.0, \text{ At } X^*=0.0 \quad \text{and} \\ \dfrac{H-h}{h} \le Y^* \le \dfrac{H}{h} \\ U^*=V^*=\dfrac{\partial\theta}{\partial X^*}=0.0, \text{ At } X^*=L/h \quad \text{and} \\ 1.0< Y^* \le \dfrac{H}{h} \\ U^*=1.0,\ V^*=0.0 \text{ and } \theta=\theta_o, \text{ At } X^*=L/h \end{array}\right\} \quad (19)$$

and $0.0 \le Y^* \le 1$.

2.2. Operating room configuration

A model for operating room with dimensions (6.0 x 6.0 x 3.0 m) is shown in fig. 1. Data taken from University Teaching Hospital in Alexandria University were inserted in this model. The main heat source was from operating table and staff and another heat source from vision Lamps. The operating table was 2.0 m length and was placed at an elevation of 75 cm, the table was centered in the room and the height for operating table was taken 55 cm. There are two groups of lamps and they were placed at 2 m from side wall and at an elevation as shown in the figure. The heat source for vision Lamps was variable; each group contains four Lamps with specification (22.7 V and 7.1 A) and may all be illuminated at the same time. The heat source is expressed in dimensionless Heat Ratio (HR). This HR. attained two values, one when half vision lamps operate HR= 0.075 and another HR =0.15 when all lamps operate. The heat source gain from operating table and staff was considered constant (HR=0.01), five persons around operating table and patient were assumed. On the other hand, the partition is H/3 from the ceiling.

We deal with the operating table and vision lamps as the solid materials with inner heat source as shown in fig. 2. The velocity

around surface for the operating table and vision lamp is very small, so can be neglected. Assume the vision lamp at constant surface temperature with inner heat source variable.
For vision lamp

$H.R.$=0.075 at half load (half lamps on),
$H.R.$= 0.15 at full load (all lamps on), (20)
U^*=0.0, V^* =0.0

And for operating table

$$H.R. = 0.01\,, \quad U^*=0.0, \qquad V^* =0.0. \tag{21}$$

Assuming no slip condition of the fluid on the partition surface, no inner heat source, temperature is uniform, steady state, neglect external force and viscous term. From these assumptions then we get: -

$$U^*= 0.0, \quad V^*= 0.0 \quad , \frac{\partial \theta}{\partial X^*} = 0.0\,, \text{ and } \quad \frac{\partial \theta}{\partial Y^*} = 0.0\,. \tag{22}$$

2.3. Numerical solution

The computer program used to solve the above problem is the finite difference technique developed by Patanker and Spalding [18] SIMPLE ALGORITHM, which is based on the discretization of the governing equation using the control differencing in space. The discretization equations were solved by the Gauss -Seidel method. The iteration method used in this program is line-by-line procedure, which is a combination of the direct method and the resulting Tri Diagonal Matrix Algorithm (TDMA).

3. Results and discussion

To obtain an effective and proper air distribution inside operating room, it was necessary to investigate many cases to understand the air distribution pattern, velocity and temperature distribution inside the operating room, and the air characteristics over the operating table. There are ten cases investigated as show fig. 3, each case study with variable parameters as Reynolds number (100-10000), and heat source for vision lamp ($H.R.$=0.075-0.15).

The results are presented in term of streamline, isothermal line, and temperature vector. The temperature vector represents the heat source location and temperature gradient. (Arrow length represents the temperature difference and direction between two adjacent grids). There are two values for aspect ratio (AR= 0.75 for the case ceiling supply and AR=0.5 for the case sidewall supply). Two values for heat generation from lamps were considered ($H.R.$=0.075 and 0.15), which correspond to partial and full illumination.

3.1. Inlet slot from side wall and exit from opposite wall near the floor (without partition)

Fig. 4 through fig. 6 represents a comparison between the airflow streamlines, isothermal lines, and heat flux gradient for different Reynolds number for cases A, B, and C which represent different inlet slot locations. In this case the aspect ratio A.R.=0.5. For fixed Reynolds number and moving inlet slot location downward, the flow pattern changed; recirculated air was reduced, the velocity above operating theater increased and the air reached the operating theater without heat addition. However, by increasing Reynolds number reverse flow increased above operating table for all inlet locations except the case that inlet slot at H/2, the air reaches directly to operating table and recirculated air occurs besides operating table.

3.2. Inlet slot from side wall at (H) and exit from opposite wall near the floor (with partition)

This section investigates the effect of hung partition for inlet slot location at height H on the velocity and temperature distribution above the operating table for different Reynolds number. The aspect ratio is A.R.=0.5 and the partition takes one position from three positions (L/4 or L/2 or 3L/4), the three cases studied are (D, E, and F), as shown in fig. 3. Figs. 7, 8, and 9 illustrated the streamlines, isothermal lines and heat flux vectors for different partition position and Reynolds number (100, 1000, 10000).

The influence of partition in modifying the flow pattern is very clear in the important region above operating table. The steep change of direction as well as the shift of circulation zone is attributed to the partition. As expected, for a fixed partition position, increasing Reynolds number effects the flow pattern and temperature distribution. At Re=100 the flow pattern is very clear, and temperature above operating table is higher at this Re number. As Re increases the recirculated air increases in the region besides operating table, and the temperature outside the recirculation regions decreases. For high Re, moving the partition position initiates eddies in the region under inlet slot location. In addition, the partition increases the air velocity and decreases the temperature in the vicinity of the partition.

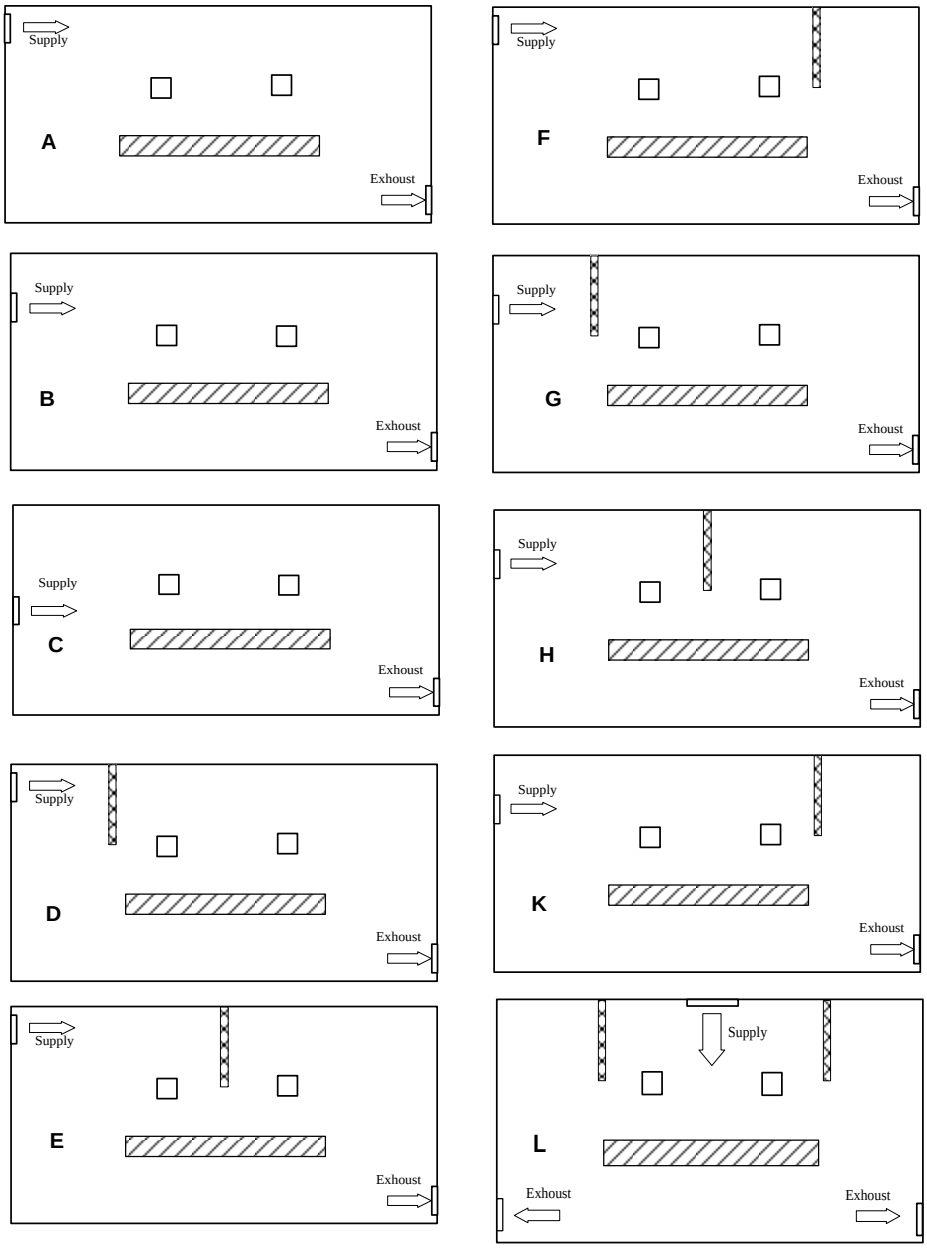

Fig. 3. Different cases study.

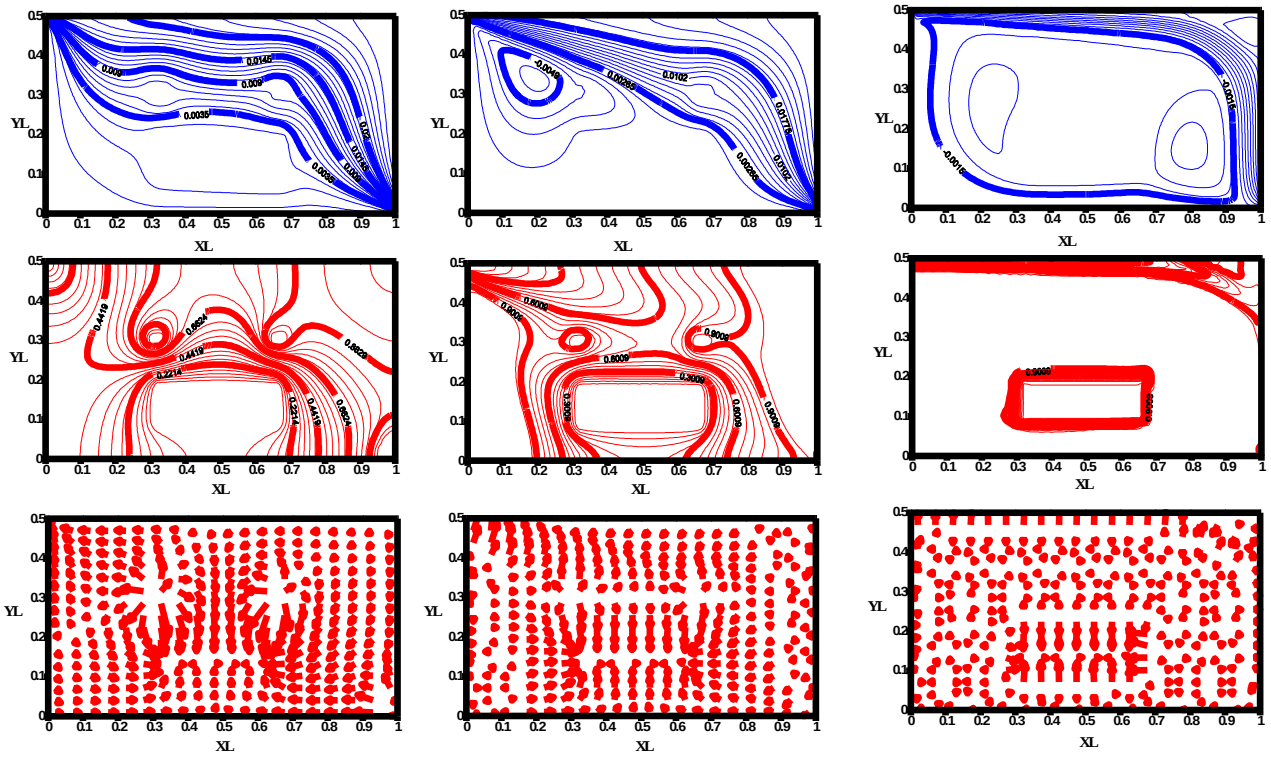

Fig. 4. Streamlines, isothermal lines and heat flux gradient for case “A” HR =0.075 and Re =100, 1000 and 10000.

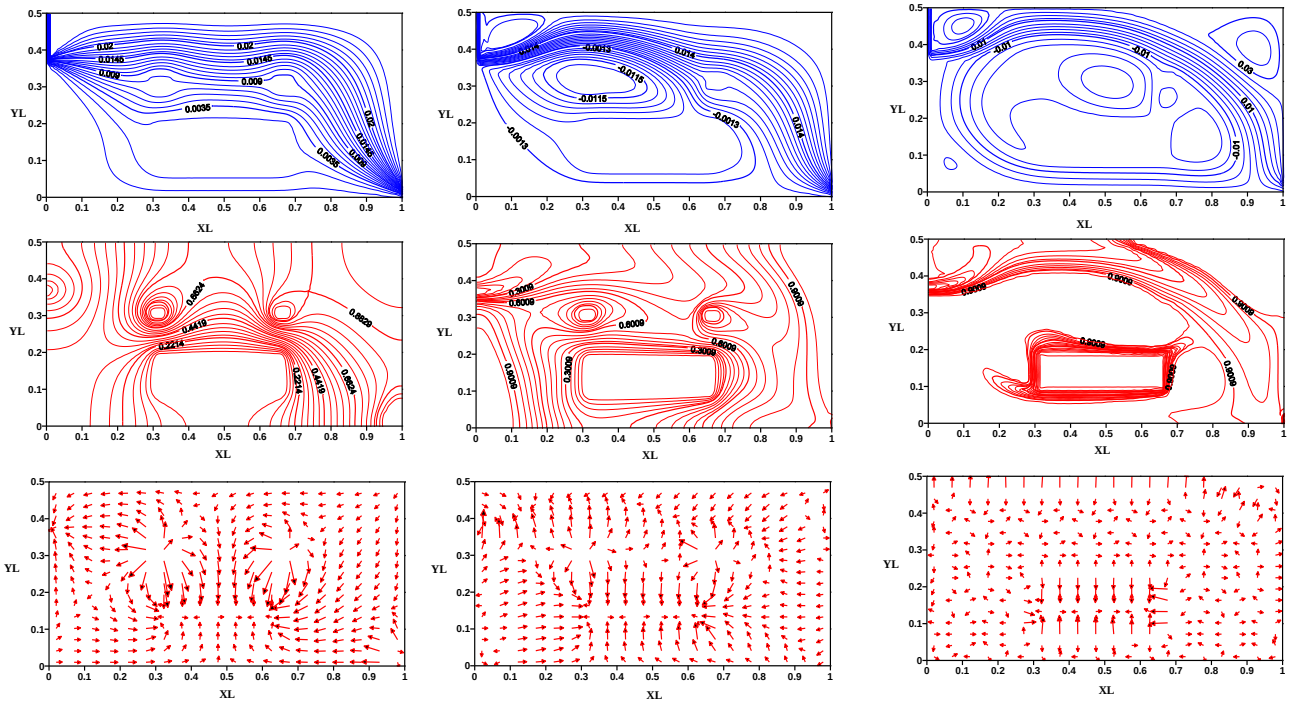

Fig. 5. Streamlines, isothermal lines and heat flux gradient for case “B” HR =0.075 and Re =100, 1000 and 10000.

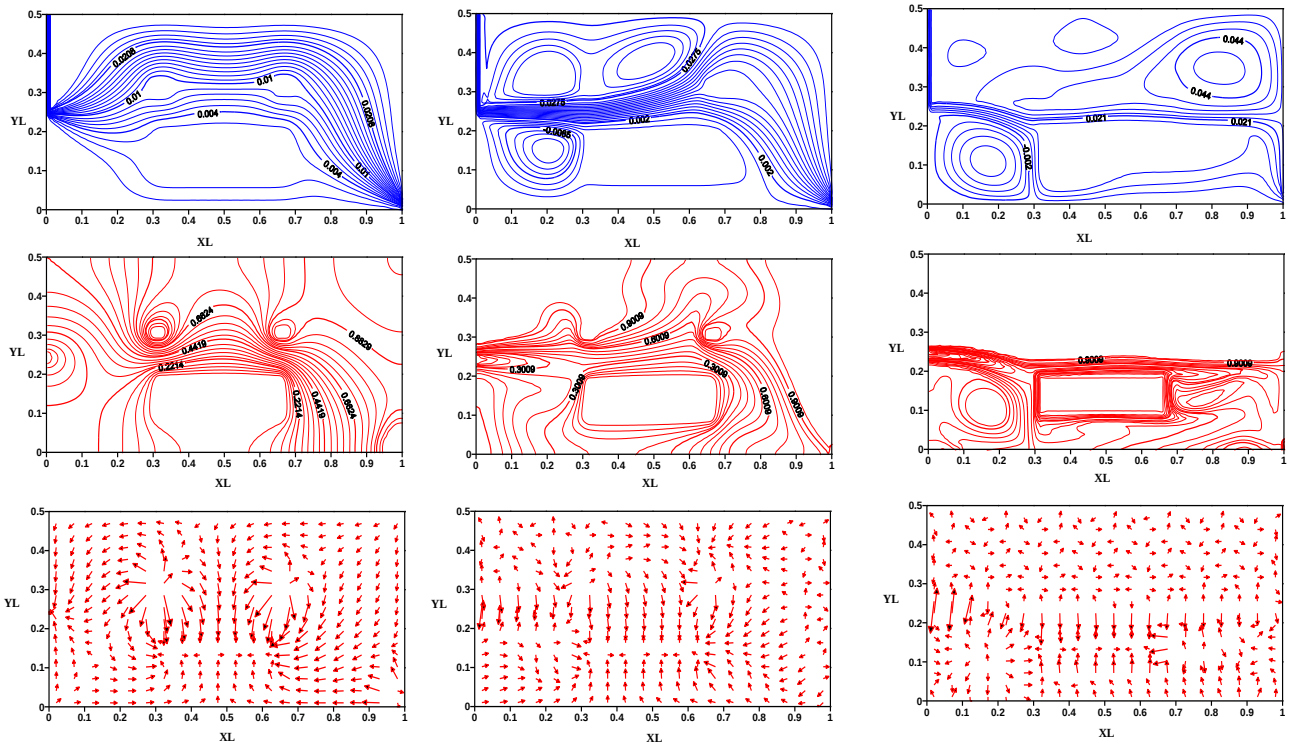

Fig. 6. Streamlines, isothermal lines and heat flux gradient for case “C” HR =0.075 and Re =100, 1000 and 10000.

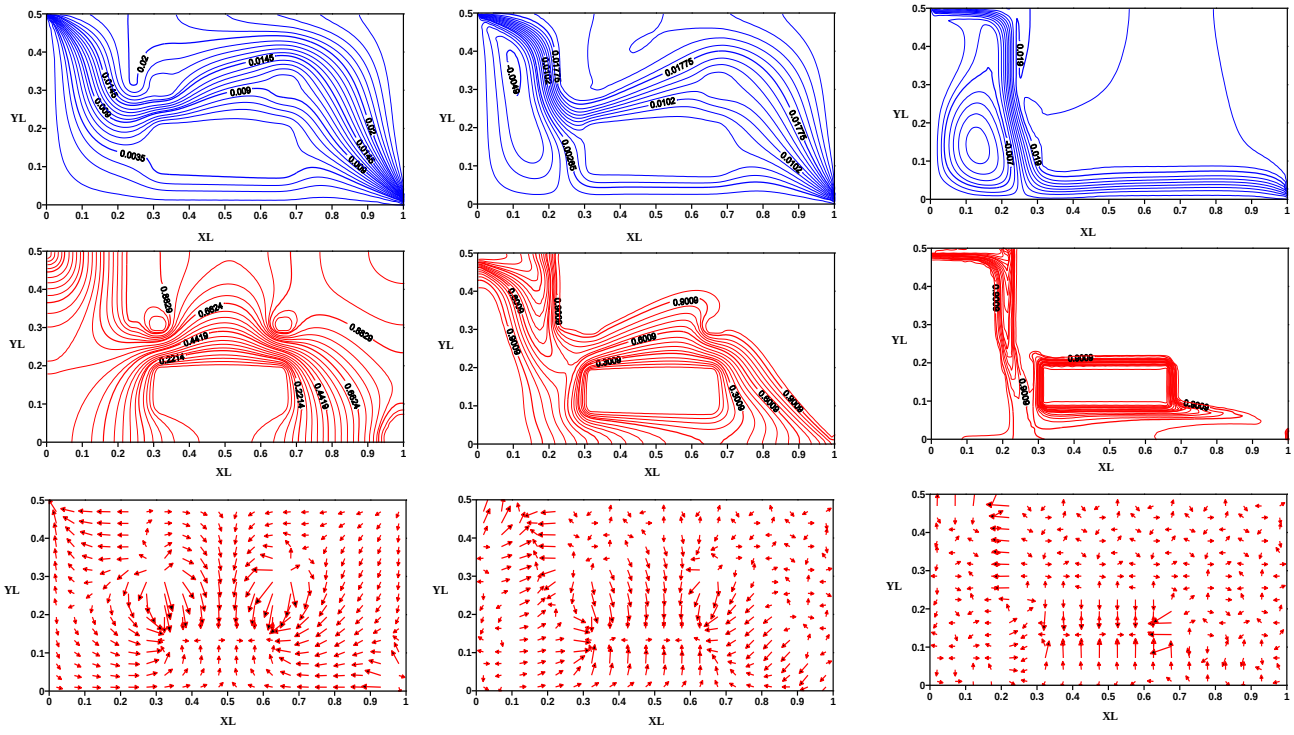

Fig. 7. Streamlines, isothermal lines and heat flux gradient for case “D” HR =0.075 and Re =100, 1000 and 10000.

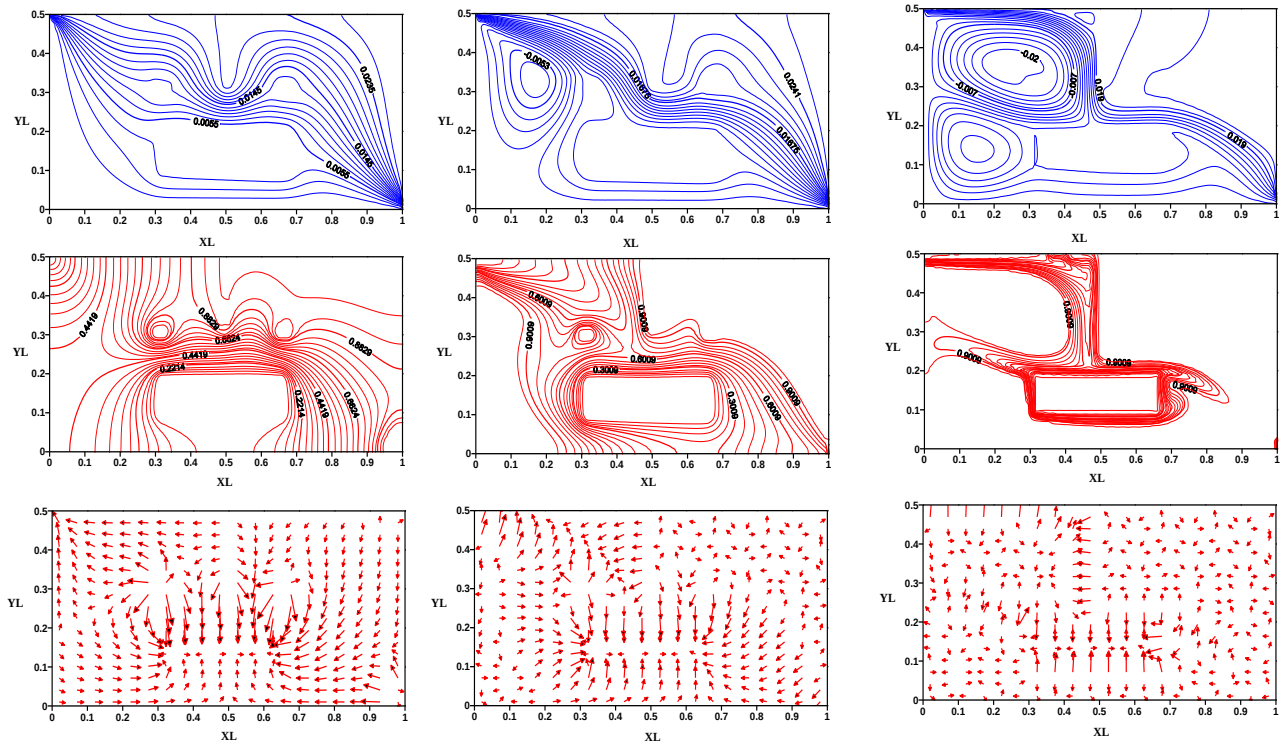

Fig. 8. Streamlines, isothermal lines and heat flux gradient for case “E” HR =0.075 and Re =100, 1000 and 10000.

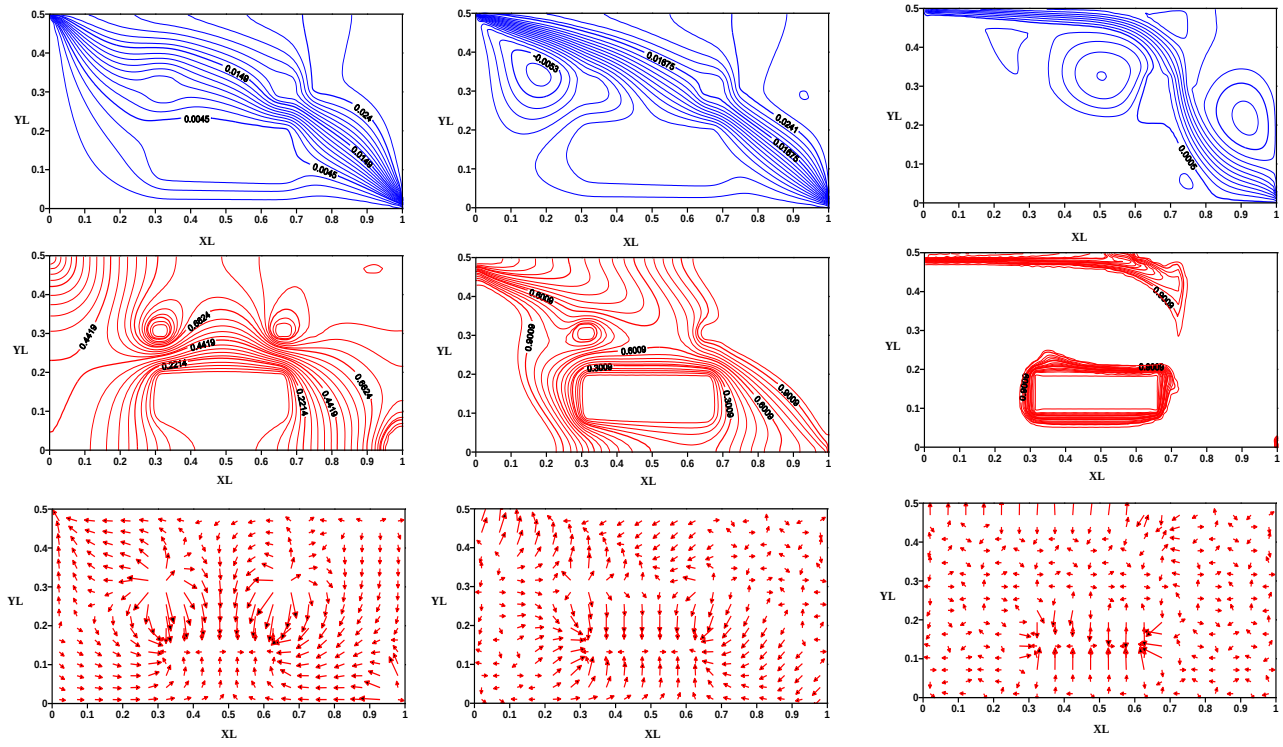

Fig. 9. Streamlines, isothermal lines and heat flux gradient for case “F” HR =0.075 and Re =100, 1000 and 10000.

3.3. Inlet slot from sidewall at (3h/4) and exit from opposite wall near the floor (with partition).

Figs. 10, 11, and 12 illustrate the flow pattern, isothermal, and temperature vector for different partition positions and Reynolds number at H.R. =0.075. The influence of the partition position on the flow pattern is similar to the previous cases. As expected, for a fixed partition position, increasing Reynolds number increases the recirculated air in the regions below and above inlet slot, and after partition. For the partition at L/4, the air after passing the inlet slot impacts the partition before vision lamp (the vision location at L/3); then a portion rises after partition and the other portion passes directly to the operating table .On the other hand, for partition at L/2 and 3/4L, the air impacted first with the vision lamp before partition, therefore the heat addition to the air increases in these cases.

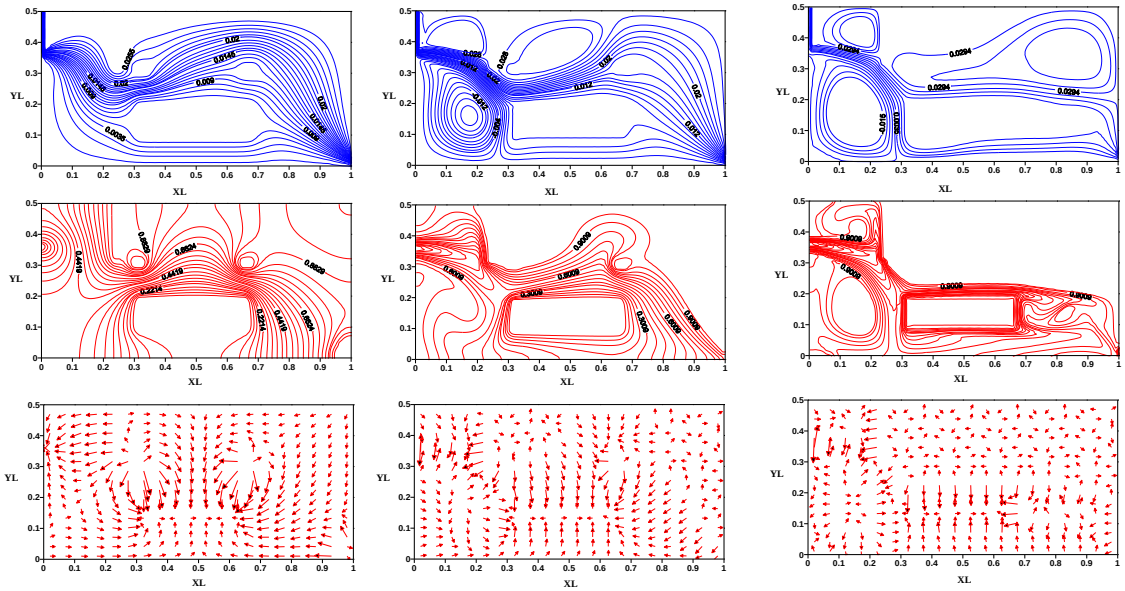

Fig. 10. Streamlines, isothermal lines and heat flux gradient for case “G” HR =0.075 and Re =100, 1000 and 10000.

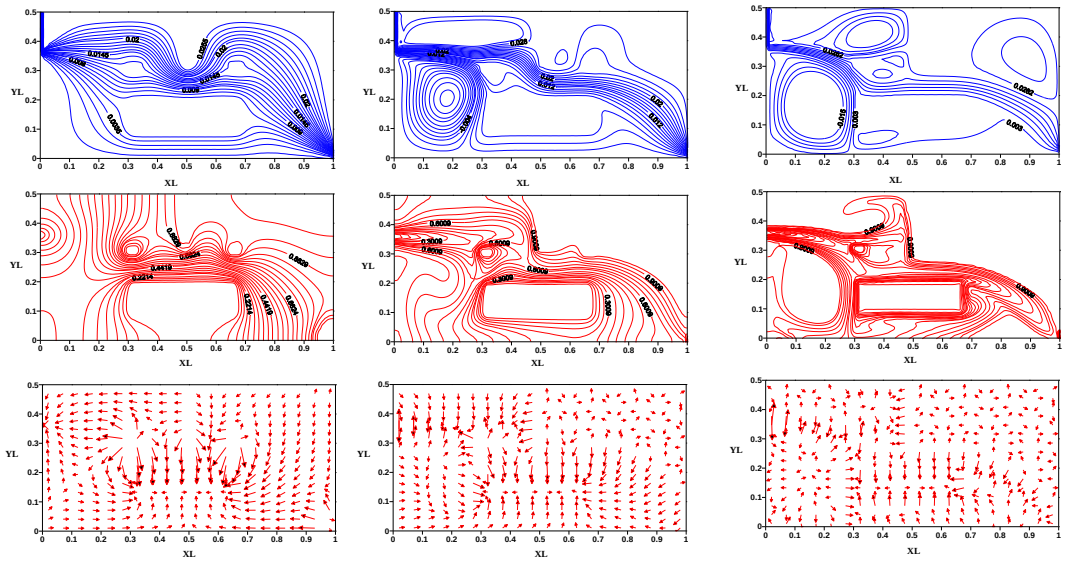

Fig. 11. Streamlines, isothermal lines and heat flux gradient for case “H” HR =0.075 and Re =100, 1000 and 10000.

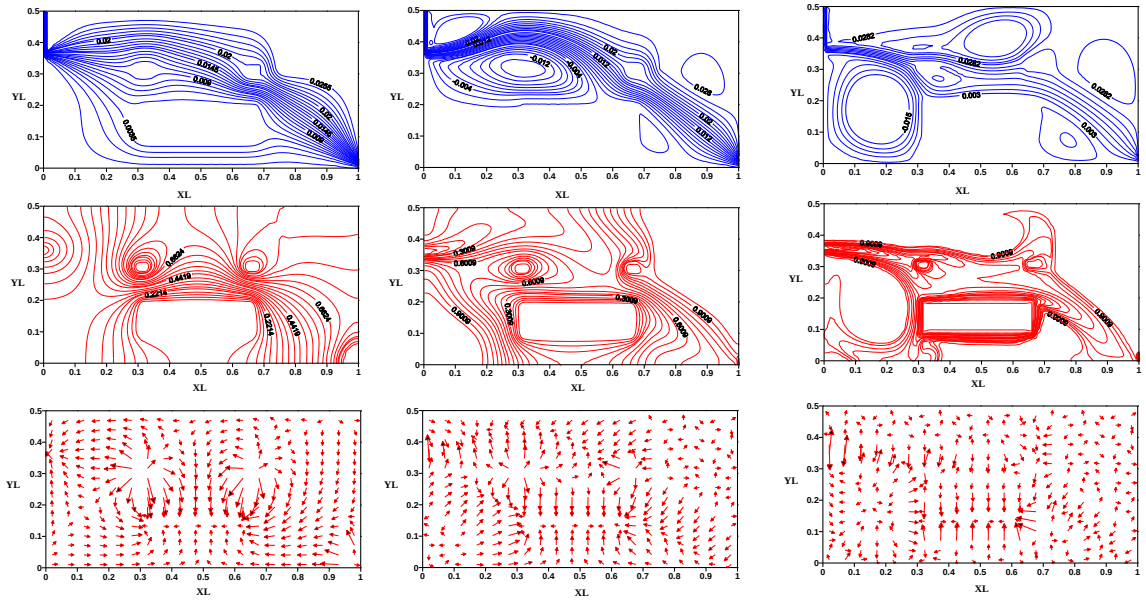

Fig. 12. Streamlines, isothermal lines and heat flux gradientfor case "K" HR =0.075 and Re =100, 1000 and 10000.

4. Design chart and selection

Figs. 13 and 14 represent design charts for velocity and temperature for a central point over the table and heat ratio *H.R.*=0.075 and *H.R.*=0.15 respectively for ten cases. From these charts we can choose the comfort condition required. Furthermore, from the required temperature above the operating table and with case design the Reynolds number can be determined. Consequently, the inlet velocity U_i is determined, and U from chart, then air velocity above the operation table from the equation $u=U*U_i$. Other wise where inlet figure with velocity required with specified case determine Reynolds number and at this Reynolds determine temperature analogous to this case.

5. Comparison with previous research

There is limited experimental work with sidewall inlet flow condition; Zhang, et al. [19]. His experimental model with dimensions 43 × 18 × 8 in, has the inlet slot from side wall at height 6.5 ″ and exit slot in the opposite wall at height 4″. The inlet supply velocity was 1.1684 m/s, Re =1000, Ar=2.15E-3, and the heat source was located at the floor with constant temperature equal 37.22 °C and inlet temperature 26 °C. The data were measured at room centerline along the height. These experiment data was converted to the present investigation model and solved numerically with the same dimensionless group that was used in this work. The results from program were compared with measurement data after converting the measuring data to dimensionless form.

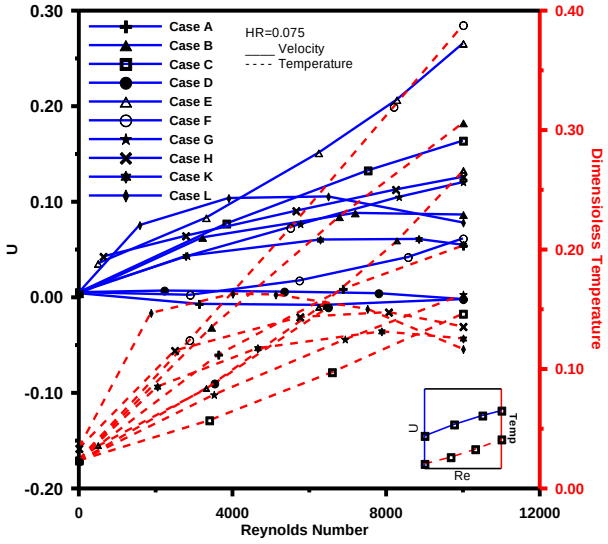

Fig. 13. Relation between velocity and temperature profiles with respect to Re for difference cases study (HR=0.075).

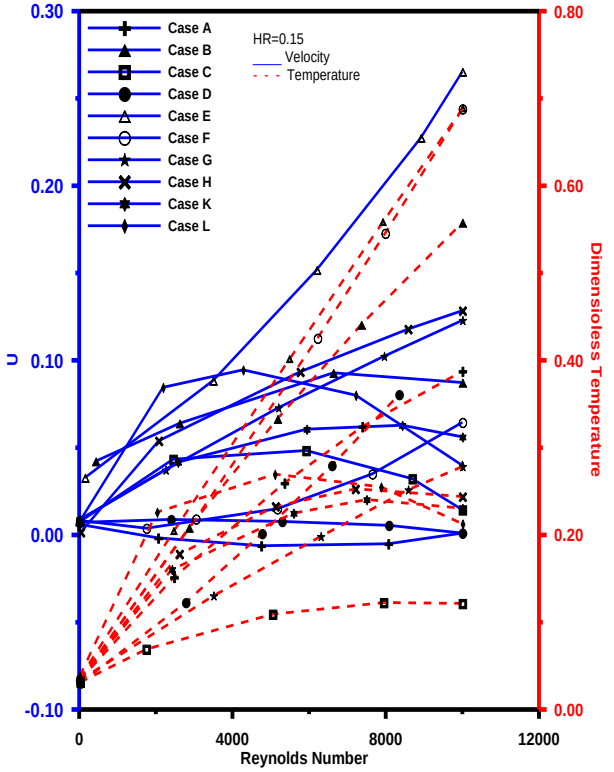

Fig. 14. Relation between velocity and temperature profiles with respect to Re for difference cases study (*H.R.*=0.15).

Fig. 15 illustrates the comparison between the present investigate and Zhang measurement. Fig. 15-a indicated the streamlines and velocity distribution, and fig. 15-b indicated isothermal lines and temperature distribution. It can be seen that there is good agreement. Present results are air velocity and temperature with measured data. The small discrepancy between the computed and measured spatial distribution of air velocity and temperature is believed to be due to the difficulty in duplicating the actual isothermal airflow condition of the experiment.

6. Conclusions

The temperature and velocity profiles were studied inside operating theater for different design and operating parameters. Different inlet location with and without partitions, the heat ratio *H.R.* =0.075 and 0.15, and different Reynolds number (100, 1000, 10000) were studied. The results, were compared with base case supply from ceiling and exit from two sidewalls near the floor with two hang partitions, that was recommended in the literature and the following results were observed: -

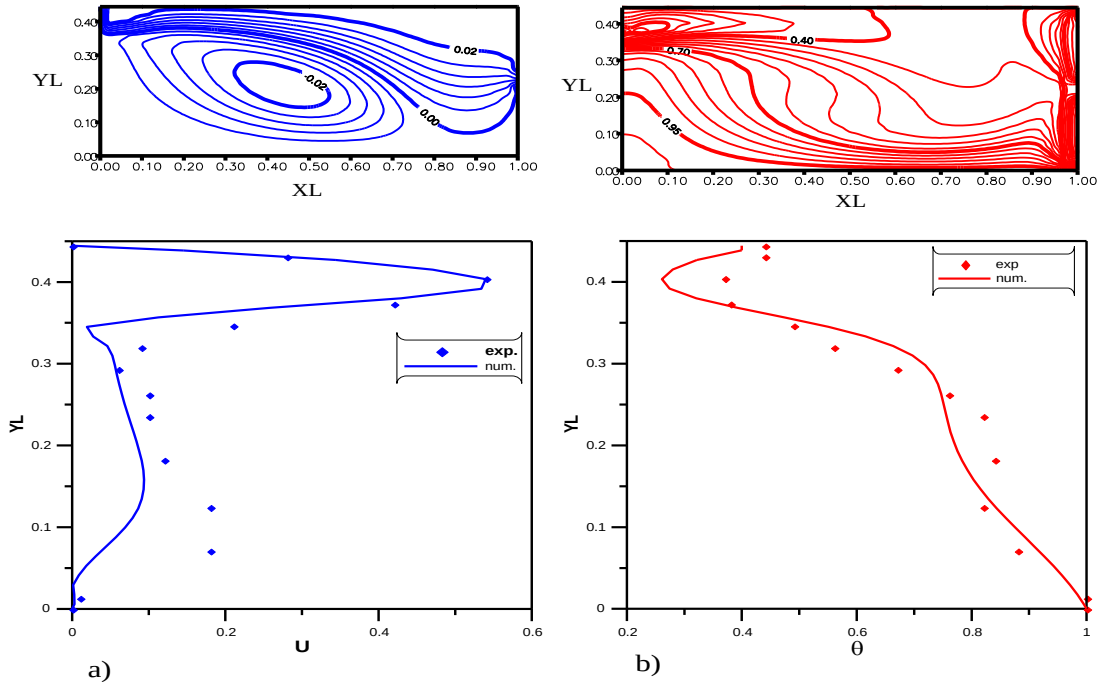

Fig. 15. Comparison between present investigations with experimental measurement by Zhang [19].

1. For different inlet locations from sidewall H and 3/4 H, it is recommended to use hang partition at position L/2.
2. For the inlet slot location H/2 the supply air reaches directly the operating table and thus it is recommended if permissible for architectural design.
3. If the space height is higher than 3 m it is recommended to use inlet air supply from the ceiling and exit from two sidewalls near the floor.

Nomenclature

Ar is the archimedes number, Gr/Re^2. (Richardson number),
AR is the aspect ratio (H/L),
c is the specific heat, kJ/kg K,
g is the gravitational acceleration, (m/s^2),
Gr is the grashof number, $g \beta (T_L - T_\infty)(h)^3 / \nu^2$,
h is the inlet slot height (m),
H is the room height (m),
$H.R$ is the heat ratio, $q\backslash\backslash h/(U \rho C \Delta T)$,
k is the thermal conductivity, W/m K,
L is the room length (m),
P is the pressure ,N/m^2 ,
Pr is the prandtl number , $\mu c/k$,
q'' is the heat generation per unit volume (W/m^3),
Re is the pure forced convection Reynolds number, hU_i/ν ,
T is the local fluid temperature, K,
T_i is the inlet air temperature, K,
T_L is the vision lamp temperature, K,
T_o is the outlet air temperature, K,
u is the local velocity in x-direction (m/s),
U_i is the inlet velocity (m/s),
U_o is the outlet velocity (m/s),
U^* is the dimensionless velocity in x-direction (u/U_i),
υ is the local velocity in y-direction (m/s),
V^* is the dimensionless velocity in Y-direction (υ/U_i),
V is the volume flow rate (m^3/sec),
X is the horizontal coordinate,
XL is the dimensionless Horizontal coordinate (X/L).
Y is the vertical coordinate, and
YL is the dimensionless Vertical coordinate (Y/L).

Greek symbols

β is the coefficient of volumetric thermal expansion ,K^{-1},
υ is the kinematic viscosity, m^2/s,
ρ is the local density, kg/m^3,
ρ_∞ is the ambient density , kg/m^3,
μ is the dynamic viscosity , Kg/m s,
θ is the dimensionless temperature $(T-T_i)/(T_L-T_i)$,
ΔP is the pressure difference between inlet and exit slots, and
ΔP^* is the pressure difference dimensionless between inlet and exit slots.

References

[1] P.L. Miller and R.T. Nash, "A Further Analysis of Room Air Distribution Performance", .ASHRAE Transaction, Vol. 77 (II), pp. 205-212 (1971).
[2] P.L. Miller and R.G. Nevins, "An Analysis of Performance of Room Air Distribution System", ASHRAE Transactions, Vol. 78 (2), pp.191-198 (1972).
[3] P.V. Nielson, "Moisture Transfer in Air Conditioned Rooms and Cold Stores Proceedings", 2d Int. CIB/RILEM Symposium, Moisture problems in buildings, Rotterdam, pp. 1-10 (1974).
[4] P.V Nielson, A. Restivo, and J.H. Whitelaw, "Buoyancy Affected Flows in Ventilated Rooms", Num. Heat Transfer Vol. 2, pp. 115-125 (1979).
[5] A.J. Baker, P.T. Williams and R.M. Kelso, "Numerical Calculation of Room Air Motion–part I, ASHRAE Transaction Vol. 100 (1), pp. 514-564 (1994).
[6] B. Vazquez, D. Samano and M. Yianneskis, "Computational Fluid Dynamics - Tool or Toy?" . UK 1st of Mechanical Engineers, Conference, pp. 57-66 (1991).
[7] Z. Jiang, Haghighat, and J.C.Y. Wang, "Thermal Comfort and Indoor Air Quality in a Partitioned Enclosure Under Mixed Convection", Journal of Building and Environment, Vol. 27 (1), pp. 77-84 (1992).
[8] Q. Chen, Z. Jiang and A. Moser, "Control of Airborne Particle Concentration and Draught Risk in an Operating Room",

BIBINF Denmark, Indoor Air, No 2, pp. 154-167 (1992).
[9] E.J. Lizardos, "Designing HVAC Systems for Optimum Indoor air Quality", Energy Engineering, Vol. 90 (4), pp. 7-29, 14 (1993).
[10] B. Vazquez, D. Samano and M. Yianneskis, "Ventilation of an Auditorium and Its Effect on Wall Heat Transfer", BIBINF UK, CIBSE, proceedings of CLIMA 2000, 1-3 November (1993), Queen Elizabeth II Conference, London, p. 325 (1993).
[11] U. Kruger, "Temperature and Velocity Distributions for Slot Devices", BIBINF UK, Air Infiltration and Ventilation Centre, 16th AIVC Conference Implementing the Results of Ventilation Research, Vol. 1, pp. 59-68 (1995).
[12] H.G. Nho and W.T. Kim, "Numerical Study on the Air Flows System with Heat Sources in an Indoor Telecommunication Room", Indoor Air '96, proceedings of the 7th International Conference on Indoor Air Quality and Climate, Nagoya, Vol. 2, pp. 1021-1026 (1996).
[13] Y. Xiaoxiong, Ch. Quingyan and L. Glicksman, "A Critical Review of Displacement Ventilation", ASHRAE Transaction V. 104 (1998).
[14] A. Fahim, "Optimization of Room Comfort Using Experimental and Numerical Modeling", Ph.D. Thesis, September Cairo University (1999).
[15] S.L. Sinha, R.C. Arora and S. Roy, "Numerical Simulation of Two-Dimensional Room Air Flow With and Without Buoyancy", .Energy and Buildings, pp. 121-129 (2000).
[16] S. Castanet, C. Beghein and C. Inard, Air Distribution in Rooms: Ventilation for Health and Sustainable Environment , Elsevier UK, Vol. 2, pp. 837-842 (2000).
[17] E.E. Khalil, "Energy Efficiency, Air Quality and Comfort In Hospitals' Operating Theatres", Proceedings of ASHRAE -Ral, Delhi, September (2004).
[18] S.V. Patankar, "Numerical Heat Transfer and Fluid Flow", New York: Hemisphere Publishing Corp. (1980).
[19] J.S. Zhang, L.L. Christianson and G.L. Riskowski, "Detailed Measurements of Room Air Distribution For Evaluating Numerical Simulation Models", ASHRAE Transactions, Vol. 98, Pt I (1992).

Received May 29, 2006
Accepted July 25, 2006